AD 697282

A UNITED STATES DEPARTMENT OF COMMERCE PUBLICATION

U.S. DEPARTMENT OF COMMERCE
Environmental Science Services Administration
Coast & Geodetic Survey

A SEISMIC STUDY OF AN UNDERWATER CHEMICAL EXPLOSION

PROJECT AMCHITKA

September 6, 1968

B. G. Reagor
D. W. Gordon

Prepared for
Advanced Research Projects Agency
Nuclear Test Detection Office
ARPA Order No. 1471

A SEISMIC STUDY OF AN UNDERWATER CHEMICAL EXPLOSION

PROJECT AMCHITKA

September 6, 1968

ARPA Order No.:	1471
ARPA Program Code No.:	9F10
ARPA Program Element Code:	62701D
Industrial Priority Rating:	DO
Name:	ESSA/Coast and Geodetic Survey Seismology Division
Date of Contract:	April 21, 1969
Principal Investigator:	James N. Jordan Special Seismological Analysis Branch (301) 49-68356 IDS 14-68356
Project Geophysicists:	B. G. Reagor D. W. Gordon

Availability

Qualified users may request copies of this document from:

Defense Documentation Center
Cameron Station
Alexandria, Virginia 22314

or

Clearinghouse
Sills Building
5285 Port Royal Road
Springfield, Virginia 22151

TABLE OF CONTENTS

TABLES

FIGURES

APPENDIX

ABSTRACT

An underwater chemical explosion was detonated 60 kilometers southwest of Amchitka Island on September 6, 1968. The device, which consisted of 250 tons of chemical explosives, was detonated at a depth of 3100 feet below sea level over the Aleutian Trench. Travel-time and amplitude data were recorded at seismograph stations throughout the United States and in Canada, Afghanistan, Australia, India, and Africa. Surface waves, however, were not detected. Travel times from the AMCHITKA explosion were late when compared to the P-wave arrivals from LONGSHOT. The average body-wave magnitude for AMCHITKA, as computed from teleseismic data, was 4.6. Significant source bias for the explosion was difficult to observe due to the limited azimuthal control. Comparative data suggest azimuthal source effects are not as significant as those associated with LONGSHOT.

INTRODUCTION

AMCHITKA, an underwater chemical explosion in the Aleutian Island region, occurred on September 6, 1968 at 02h 07m 10.4s U.T. Geographic coordinates were 51°07'30.0" North, 178°22'00.0" East, a position approximately 60 kilometers southwest of Amchitka Island in the Rat Islands group. The explosive device consisted of a container packed with 250 tons of high-explosive material which was towed to the shot area, sunk, and detonated at a depth of 3100 feet below sea level.

LONGSHOT, a nuclear device exploded on Amchitka Island in 1965, showed striking azimuthal variations in travel times and amplitudes recorded on distant seismographs. In this report, the results of the AMCHITKA explosion are compared with those from LONGSHOT to determine the effect of shifting the shot point from the axis of the Aleutian Island arc to a position over the adjacent trench.

The World-Wide Network of Standard Seismographs (WWNSS), the Long Range Seismic Measurements (LRSM) stations, and the Canadian National Network were the principal sources of data for this report. Basically, the WWNSS and LRSM instrumentation are similar: 3-component short-period Benioff systems and 3-component long-period (Sprengnether) systems. However, there are significant differences between the short-period and long-period response of the two systems. The WWNSS short-period response is maximum at 0.6 sec. In contrast, the corresponding LRSM system peaks between 0.3 and 0.4 sec. The WWNSS long-period system has a broad-band response with a peak amplification in the 15- to 20-sec period range, while the LRSM has a narrower passband with maximum magnification at about 25 sec. The Canadian Network uses Willmore short-period and Columbia long-period instruments. The peak response for the short periods is 0.4 to 0.5 sec, while the long-period response curve is maximum in the 15-sec period range. Short-period response curves representing the three systems are compared in Appendix 1. Appendix 2 illustrates the corresponding long-period systems. The curves shown in the figures are typical of the response configuration; however, it should be noted that peak instrument magnifications vary from station to station.

This data was supplemented by information furnished by university stations and other C&GS and cooperating stations where instrumentation varys from a single short-period seismometer to an array of instruments. In general, instrumentation is similar to WWNSS equipment, although it may not be as complete or as recently calibrated.

GEOLOGICAL ENVIRONMENT

The source region, which consists of deep sea trenches and parallel chains of volcanic islands, exemplifies the characteristics of a Pacific-type arcuate structure. These structures are associated with large gravity anomalies and high seismic activity. The Aleutian trench (Murray. 1945), a narrow depression in the ocean floor paralleling the Aleutian Islands, extends from Attu Island in the Western Aleutians to the Yakutat Bay area in the Gulf of Alaska, a distance of over 2000 miles. The trench, which is 50 to 100 miles wide and extends to a depth of over 25,000 feet, can be divided into three parts: (1) North slope; (2) south slope; and (3) trench floor. The north or continental slope of the trench is defined between the 100-fathom contour and the trench floor. The continental slope (Murray, ibid), which is characterized by an average slope of 3° to 4°, is indented by numerous submarine valleys, terminating at depths ranging from 2000 to 4000 fathoms. In contrast, the south slope is relatively smoother and has an average slope of 1° to 2°. The trench floor occupies an area of 20 to 70 miles from the edge of the continental slope and lies 1200 to 9600 feet below the adjacent Pacific Ocean floor on the south. The trench floor is underlain by approximately 2 kilometers (Shor, 1964) of thinly bedded horizontal sediments which contain high-angle faults with evidence of recent small movements (Ewing, et. al., 1965). The trench is well delineated eastward, in the vicinity of Cape St. Elias, where its edge is marked by the 2000-fathom contour. Traces of the trench probably extend across the Continental Shelf to Yakutat Bay. Westward from Cape St. Elias, the floor steadly descends to an estimated depth of 3900 to 4200 fathoms. Toward the east, the trench parallels the island chain, which nearly coincides with the arc of a circle with a radius of 1400 miles (Murray, 1945).

Basically, the Aleutian Island Ridge is composed of pre-middle Tertiary rocks and subordinate amounts of upper Tertiary coarse clastic sediments and subaerial lava flows (Eardley, 1962). Gates and Gibson's (1956) structural interpretation suggests the western part of the Aleutian Ridge is an arched and faulted asymmetrical wedge, bounded by northward-dipping normal faults on the north and by a northward-dipping zone of reverse faults on the south. In their study of the 1965 Rat Island aftershocks, Jordan, et. al., 1965B, observed that the limits of aftershock activity were sharply defined to the east and west of the Rat Island group, and suggested that north-south trending fracture zones divide the island chain into large fault blocks.

Based on refraction profiles, Shor (1964) estimated a depth of 22 kilometers to the Mohorovicic discontinuity beneath the islands. This compares favorably with Carder's (Carder, Tocher, et. al., 1966) estimate of 25 kilometers computed from LONGSHOT data.

DATA

Travel-time and amplitude data associated with the AMCHITKA explosion were measured from 34 seismographs representing the WWNSS, LRSM, Canadian networks, and C&GS cooperating stations. In addition, travel-time data were provided by 17 stations where the recorded signal was too emergent for accurate measurements, or where instrument calibration is not performed routinely. The most distant known record of the seismic signal was written at Windhoek, South Africa at 148 degrees, and the nearest station was on Adak Island, 3.2 degrees from the shot point. The basic seismic data made available by this investigation are summarized in Table 1, which includes station arrival times (corrected for ellipticity and elevation), amplitudes and periods of selected phases, and C&GS body-wave magnitudes (m_b). Travel-time residuals (O-C), which are also shown in the table, refer to the Jeffreys-Bullen (1948) surface focus curve. Figure 1 shows the locations of North American stations which recorded the explosion. In addition to these stations, the seismic signal was recorded at six overseas sites--two in Asia; two in

Australia; and two in Africa. Instrumental magnification, which relates to signal detection, is plotted as a function of distance in Figure 2 which indicates that instruments below a magnification level of 25,000 did not record the explosion.

In contrast with the widely recorded LONGSHOT data, seismic signals recorded from the AMCHITKA explosion are limited primarily to the P-wave arrival times. Following the P-wave arrival, a series of pulses was observed on some seismograms which gave the appearance of a "ringing effect." These pulses have been observed from previous water experiments and may be attributed to ocean-bottom multiples. The multiple arrivals observed on the seismograms occur at 4- to 6-sec intervals. Based on the travel time of energy reflected between the water surface and the trench floor, an interval of 5.4 sec was obtained. This agrees closely with the observed intervals. Other widely recorded phases from LONGSHOT, such as Pg and Lg, were, if recorded, unrecognizable at close stations for the AMCHITKA explosion. Rayleigh waves generated by the explosion were not detected.

The majority of data was limited to the first quadrant, which corresponds to reception at Canadian and United States stations. Out of a total of 49 stations in the direct P-distance range, only four stations represent the third and fourth quadrants. The most distant signal reception, at Windhoek (WIN) and Pretoria (PRE), South Africa, is associated with the caustic in the PKP travel-time curve at approximately 145 degrees.

TRAVEL TIMES

Two graphs have been prepared to show travel-time results over the P-wave range. Figure 3 shows the observed travel times with reference to a 8.1 km/sec velocity and Jeffreys-Bullen (1948) surface-focus curve. Travel-time residuals (O-C) with respect to the Jeffreys-Bullen curve are plotted in Figure 4 which covers the distance range beyond 3000 kilometers. Inspection of the two graphs reveals that nearly all travel times are early with respect to Jeffreys-Bullen values. Experience gained from large nuclear explosions has indicated that Jeffreys-Bullen surface-focus times are approximately 2 sec late in the range beyond 20 degrees (Gutenberg and Richter, 1964; Burke-Gaffney and Bullen, 1957; Carder, Gordon, and Jordan, 1966). The average Jeffreys-Bullen residual for the AMCHITKA event is -1.1 sec, which implies that the travel times are late when compared to average travel times compiled from large explosions. However, consideration of the shot depth and the column of water beneath the shot point indicates a delay of approximately 1 sec due to burial and the velocity contrast between water and rock.

Thus, AMCHITKA travel times are approximately the same as average values from explosions if corrections are made for the shot depth and source medium.

In contrast, the average Jeffreys-Bullen residual associated with LONGSHOT, which was located circa 60 kilometers from the AMCHITKA site, was -3.4 sec, infering that LONGSHOT times are about 1 to 1½ sec earlier than the AMCHITKA explosion even after corrections for water transit time and for the +2 sec in the Jeffreys-Bullen tables for surface focus. It is evident that regional effects at the source play an important part in travel times. Chinnery and Toksoz (1967) suggested that early travel times associated with LONGSHOT are due to high-velocity material in the upper mantle beneath the Aleutian arc.

Figure 5 shows Jeffreys-Bullen residuals for LONGSHOT and AMCHITKA travel times recorded at common stations. Results from stations less than 20 degrees from the shot locations are widely scattered. For example, Adak Island (ADK) is relatively late (-1.7 sec) for LONGSHOT and very near the average residual from AMCHITKA. Conversely, Kodiak (KDC) is anomalously early for LONGSHOT and only slightly early for AMCHITKA and

Tanana (TNN) is about 1½ sec late for both events. However, beyond 30 degrees, the residuals generally indicate relatively late or early readings at the same station which also reflects the importance of regional effects of travel-time variations near the receiver. For example, College (COL) residuals infer arrivals approximately ½ sec early for both test shots. The Las Cruces, New Mexico (LC-) value is anomalously late for the AMCHITKA shot. This may be an interpretation error due to low signal-to-noise conditions on the records of the smaller shot. Table 2 contains Jeffreys-Bullen residuals at distant stations which received both events. In this table, regional patterns in the residuals have been revealed by grouping the residuals according to tectonic province. As indicated in studies of upper mantle and crustal velocities (Pakiser and Zietz, 1965), regional effects associated with the Western Mountain environment indicate travel-time delay relative to the Eastern United States. Although the AMCHITKA data conform to the velocity patterns across the United States, it is suspected that the anomalously early values for LONGSHOT recorded in the Appalachian region are a manifestation of pronounced lateral inhomogeneity at the source.

AMPLITUDES

Amplitudes of the maximum motion in the first three cycles of AMCHITKA signals are shown in Figure 6. A very emergent beginning and a period of about 0.6 sec characterized the onset of the P wave on the seismograms. Signals written at stations with high instrument magnifications contained high-frequency phases which were not seen at lower gain levels. Selected representative signals from the AMCHITKA explosion, at varying distances and instrumental magnifications, are illustrated in Figure 7.

Figures 8 and 9 are plots of observed AMCHITKA and LONGSHOT P-wave ground amplitudes as a function of distance. The reference lines on the figures represent amplitudes predicted by the Gutenberg and Richter (1956) attenuation factors corresponding to the average body-wave magnitudes of LONGSHOT (6.0) and the AMCHITKA event (4.6). Similarities, as well as differences, are observed between the two graphs. At distances less than 20 degrees, LONGSHOT amplitudes are low relative to AMCHITKA at the same stations. In the 40-degree range, the data for LONGSHOT, generally obtained from Canadian stations, do not support the amplitude high predicted by the empirical curve. Amplitudes in the 45- to 55-degree range, which covers reception at stations in the contiguous United States, generally show station correlation. Similar results are evident between 60 and 70 degrees where amplitudes tend to exceed expected values.

MAGNITUDES

AMCHITKA body-wave magnitudes representing individual stations are plotted in Figure 10 with reference to a 4.6 m_b, the average teleseismic magnitude. Body-wave magnitude, in this report, refers to C&GS P-wave magnitude:

$$m_b = \log (A/T) + Q$$

where

A = ground amplitude in microns

T = corresponding period

Q = distance attenuation correction.

The scatter observed in the figure is typical of the precision of magnitude measurements. In addition to measurement errors, the variations are probably associated with (1) bias in the assumed amplitude-distance relationship; (2) asymmetric energy radiation at the source; (3) attenuation differences along the transmission paths; and (4) variations in the ground response at the recording stations.

Magnitude residuals (individual station magnitude-average magnitudes) are listed in Table 3 for stations which recorded both AMCHITKA and LONGSHOT. In the table, data are grouped according to tectonic provinces. In view of the scatter exhibited by the data, the means associated with the various groups are not statistically significant. However, the differences between LONGSHOT and AMCHITKA residuals at the same station tend to be less than the overall scatter. These results also show general correlation with the findings of Jordan, et. al., 1965A, who plotted P-wave amplitude patterns associated with Algerian and Kazak events recorded at United States stations. For example, Eureka, Nevada (EUR) registered higher than expected amplitudes for both events as well as both test shots. The region of the Great Plains surrounding LASA in Montana also registered higher amplitudes than predicted by the average event and test shot magnitudes. In general, the Western Orogenic Belt showed amplitudes less than expected, whereas the Central Stable Interior and the Appalachian Belt indicated higher amplitudes than expected for both shots.

Surface-wave magnitudes are also of particular interest to the Vela Uniform participants due to the observed difference between the relative excitation of surface waves by earthquakes and explosions.

In April 1968, the C&GS initiated a program to obtain surface-wave data on a routine basis for inclusion in the PDE program. The C&GS computes the surface-wave magnitudes (M_S) with the use of the formula

$$M_S = \text{Log}_{10}\ A/T + 1.66\ \text{Log}_{10}\ \Delta^{\circ} + 3.3$$

where A, the horizontal ground amplitude in microns, corresponds to the maximum 18- to 22-sec (T) wave measured on long-period seismograms.

To examine the relationship between m_b and M_S for earthquakes and explosions, earthquakes which occurred within the same geographical and tectonic region as LONGSHOT and AMCHITKA are plotted in Figure 11. The points on the graph represent three different comparisons of m_b versus M_S: (1) Individual station magnitudes for earthquakes routinely reported to the PDE program for the past 1½-year period; (2) average earthquake magnitudes (Liebermann, et. al., 1966); (3) individual station magnitudes for LONGSHOT computed from the Canadian Network (Currie, 1967) and the LRSM (Clark, 1966) Network. The surface-wave magnitudes were measured, for both the Canadian and LRSM data, from the vertical long-period component. The Canadians determined M_S by Bath's (1952) formula, whereas the LRSM used the same formula as C&GS but with modifications to permit wave periods less than 18 sec to be used. The relationship between m_b and M_S, determined by Gutenberg and Richter (1956) and Romney (1963), is added to the graph for comparison purposes. Investigations of LRSM data by Romney (ibid) show that $m_b = M_S$ for earthquakes. From the graph, however, the individual magnitudes are widely scattered above and below the line. The empirical relationship given by Gutenberg and Richter (ibid) appears to fit the average earthquake magnitude values, and beyond 5.8 m_b, the individual magnitudes appear to have a corresponding trend. The two linear relationships intersect at a m_b of 6.8. The LONGSHOT magnitudes are observed to lie below both reference lines. The surface-wave magnitudes are about an order less than the associated body-wave magnitude for each individual station. Collectively, the average m_b for LONGSHOT (5.9) would, based on the Gutenberg and Richter (ibid) curve, generate a 5.4 M_S. However, the average M_S computed for LONGSHOT was 4.2 which corresponds to a 5.1 m_b earthquake. Although the AMCHITKA explosion did not produce any measurable surface waves, the average teleseismic m_b of 4.6 corresponds to an earthquake surface-wave magnitude of 3.4.

These observations indicate that earthquakes of comparable body-wave magnitude, located in the same geographical and tectonic region, generate larger surface waves than those produced by LONGSHOT. This statement supports earlier conclusions that explosions do not excite the long-period part of the seismic spectrum as compared to earthquakes (Liebermann, et. al., 1966). Also, surface-wave magnitudes of earthquakes are not consistently larger than the corresponding body-wave magnitude.

HYPOCENTRAL COMPUTATIONS

The results of the computer solutions carried out using the C&GS hypocenter program (Engdahl and Gunst, 1966), are shown in Table 4. The computations were performed with the use of the standard travel-time tables of Jeffreys-Bullen (1948) and the recently published Herrin tables (Herrin and Taggart, 1968A). The first entry contains the given coordinates of the shot, and the remaining lines refer to computer solutions carried out in several different modes. These include a conventional computer solution (2) with focal depth unrestrained, and solutions (3, 4) with depth restrained to surface focus. Entries 5 and 6 are computations with arrival times adjusted on the basis of LONGSHOT residuals, i.e., in these cases, LONGSHOT results were used as a calibration shot. The reading from Adak Island at about 350 kilometers distance was included in all computations.

The accuracy of the computer solutions which are based on P-wave arrivals is limited by the observed times, azimuth control, the validity of the travel-time curves used, and by anomalous conditions at the source and receivers. The C&GS program also computes standard errors which reflect the precision or internal consistency of the data. Standard errors of latitude and longitude (the intercepts of the error ellipse with the coordinate lines of the computer epicenter) were approximately ±5 kilometers for AMCHITKA solutions restrained to surface focus.

With the depth parameter restrained to zero kilometer, the epicenter of the AMCHITKA explosion, based on observed arrival times and using both the Jeffreys-Bullen and Herrin curves (solutions 2 and 4), was consistently shifted toward the northwest with a corresponding alteration of the origin time (Table 4). As observed earlier in this report, the average arrival times relative to the standard Jeffreys-Bullen tables were approximately 1 sec early. A separate computer run using the Herrin curve with all source coordinates restrained indicated an average residual of +1.6 sec, which is approximately 1 sec late when the computed delay transit time associated with the water column above and below the shot point is considered.

LONGSHOT, as determined by normal location procedures, was shifted approximately 25-30 kilometers northwest of the true epicenter. Douglas (1967) indicates the shift was caused by a regional bias in travel times in the Aleutian region as revealed by the travel-time residuals associated with the known source coordinates. Herrin and Taggart (1968B) also found that LONGSHOT showed a significant travel-time bias. At equivalent distance, travel times were 2½ sec greater to the south than to the north. They attributed the observed azimuthal variation in travel times to a layer of high-velocity material with a northerly dip. It has been suggested (Oliver and Isacks, 1967) that such layers, downwarped portions of the lithosphere 50 to 100 kilometers thick, are characteristic of island arc structure.

Consideration of epicentral errors has indicated that the velocity structure of the crust and upper mantle of specific sources may decrease or delay travel time relative to standard curves designed to represent average conditions. In addition, azimuthal variations in velocity at equivalent depth introduce source bias. Although the uncorrected computer solutions for AMCHITKA gave results similar to LONGSHOT computations, it is difficult to examine bias associated with AMCHITKA due to the lack of azimuthal control. However, it is very possible that the shift of the shot point from the ridge to the trench has significantly reduced the azimuthal variation in the length of travel path through the anomalous layer.

The proximity of the AMCHITKA explosion to that of LONGSHOT suggested an adjustment of the AMCHITKA arrival times by the residuals observed from LONGSHOT. Following the method outlined by Herrin and Taggart (1963), arrival times from AMCHITKA and the true residuals from LONGSHOT were added algebraically. The results of the computations carried out with the Jeffreys-Bullen curve are given by solution 5, where depth was treated as an unknown, and solution 6, which restrains depth to surface focus. In trials 5 and 6, the northerly shift of the epicenter was 25 to 50 percent of that corresponding to uncorrected arrival times, indicating that application of calibration shot data reduced the epicenter error considerably.

SUMMARY OF OBSERVATIONS

1. Travel times show that AMCHITKA arrival times are relatively early with respect to the standard Jeffreys-Bullen curve, but later than LONGSHOT travel times. AMCHITKA travel times, if corrections are made for shot depth and source medium, relative to average values from explosions show: (1) They are approximately the same; (2) they are later than LONGSHOT travel times by about 1 to 1½ sec.

2. An analysis of seismograms of the AMCHITKA explosions infers ocean-bottom multiples occur at 4- to 6-sec intervals. The computed reverberation interval is 5.4 sec.

3. Magnitude residuals for both shots show amplitudes less than expected for the Western United States, whereas amplitudes are higher for the Eastern United States.

4. Both shots substantiate previous observations that surface waves associated with explosions are smaller than those associated with earthquakes of comparable body-wave magnitudes. In the case of LONGSHOT, a 5.9 m_b and a 4.2 M_S were observed. Using Gutenberg

and Richter linear relationship, a M_S of 4.2 would correspond to an earthquake m_b of 5.1. Surface-wave data were not available from the AMCHITKA explosion.

5. Computer solutions carried out with the Jeffreys-Bullen and Herrin curves located the epicenter approximately 20 kilometers northwest of the shot point. The Herrin average residual, with all parameters restrained, was approximately 1 sec late when the water travel-time delay was applied.

6. Calibration of the AMCHITKA explosion using residuals from LONGSHOT gave an epicenter about 5 kilometers from the given location.

7. A clear statement about source bias associated with the AMCHITKA explosion cannot be made due to poor azimuthal control. Comparative data suggest that the source bias prominently identifiable with LONGSHOT has been reduced.

REFERENCES

Bath, M., 1952, "Earthquake Magnitude Determination from the Vertical Component of Surface Waves," Trans. Amer. Geophys. Union, No. 33, pp. 349-364.

Burke-Gaffney, T.N. and Bullen, K.E., 1957, "Seismological and Related Aspects of the 1954 Hydrogen Bomb Explosions," Australian Journal of Physics, Vol. 10, pp. 130-136.

Carder, D.S. and Bailey, L.F., 1958, "Seismic Wave Travel Times from Nuclear Explosions," B.S.S.A., Vol. 48, pp. 377-398.

Carder, D.S., 1964, "Travel Times from Central Pacific Nuclear Explosions and Inferred Mantle Structure," B.S.S.A., Vol. 54, No. 6, Part B, pp. 2271-2294.

Carder, D.S., Gordon, D.W., and Jordan, J.N., 1966, "Analysis of Surface-Foci Travel Times," B.S.S.A., Vol. 56, No. 4, pp. 815-840.

Carder, D.S., Tocher, D., Bute, C.G., Stewart, S., Eisler, J.D., and Berg, E., 1966, "Seismic Wave Arrivals from LONGSHOT 0° to 25°," ARPA Air Force Grant Order No. 533.

Chinnery, M.A. and Toksoz, M.N., 1967, "P-wave Velocities in the Mantle Below 700 Kilometers," B.S.S.A., Vol. 57, pp. 199-226.

Clark, D.M., 1966, "Long Range Seismic Measurements-LONG SHOT," Seismic Data Laboratory Report No. 133, UED Earth Sciences Division, January 1966.

Cleary, J.R. and Hales, H.L., 1966, "An Analysis of the Travel Times of P Waves to North American Stations, in the Distance Range 32° to 100°," B.S.S.A., Vol. 56, No. 2, pp. 467-489.

Cleary, J.R. and Hales, A.L., 1966, "Azimuthal Variation of United States Station Residuals," Nature, Vol. 210, pp. 619-620.

Currie, R.G., 1967, "A Comparison of LONGSHOT and Earthquakes," ARPA Air Force Grant No. AF-AFOSR-1022-66.

Douglas, A., 1967, "Joint Epicentre Determination," Nature, Vol. 215, pp. 47-48.

Eardley, A.J., 1962, "Structural Geology of North America," 2nd Edition, Harper, New York, 743 pages.

Engdahl, E.R. and Gunst, R.H., 1966, "Use of a High Speed Computer for the Preliminary Determination of Earthquake Hypocenters," B.S.S.A., Vol. 56, pp. 325-336.

Ewing, M., Ludwig, W.J., and Ewing, J., 1965, "Oceanic Structural History of the Bering Sea," J. Geophys. Res., Vol. 70, No. 8, pp. 4593-4600.

Gates, O. and Gibson, W.M., 1956, "Interpretation of the Configuration of the Aleutian Ridge," Bull. Geol. Soc. Am., Vol. 67, pp. 127-146.

Green, R.W.E. and Hales, A.L., 1968, "The Travel Times of P Waves to 30° in the Central United States and Upper Mantle Structure," B.S.S.A., Vol. 58, No. 1, pp. 267-289.

Gutenberg, B., 1945, "Amplitudes of Surface Waves and Magnitudes of Shallow Earthquakes," B.S.S.A., Vol. 35, pp. 3-12.

Gutenberg, B. and Richter, C.F., 1956, "Magnitude and Energy of Earthquakes," Annali di Geofisica, Vol. IX, pp. 1-15.

Gutenberg, B. and Richter, C.F., 1964, "Seismic Waves from Atom Bomb Test," Trans. Amer. Geophys. Union, Vol. 72, pp. 776.

Hales, A.L., Cleary, J.R., Doyle, H.A., Green, R., and Roberts, J., 1968, "P-wave Station Anomalies and the Structure of the Upper Mantle," J. Geophys. Res., Vol. 73, No. 12, pp. 3885-3896.

Herrin, E. and Taggart, J., 1962, "Regional Variations in Pn Velocity and Their Effect on the Location of Epicenters," B.S.S.A., Vol. 52, No. 5, pp. 1037-1046.

Herrin, E. and Taggart, J., 1963, "The Use of Calibration Shots in the Determination of Hypocenters," ARPA Air Force Grant No. AFOSR-61-137.

Herrin, E. and Taggart, J., 1968A, "Regional Variations in P-Travel Times," B.S.S.A., Vol. 58, No. 4, pp. 1325-1337.

Herrin, E. and Taggart, J., 1968B, "Source Bias in Epicenter Determinations," B.S.S.A., Vol. 58, No. 6, pp. 1791-1796.

Isacks, B. and Oliver, J., 1968, "Seismology and the New Global Tectonics," J. Geophys. Res., Vol. 73, No. 18, pp. 5855-5899.

Jeffreys, H. and Bullen, K.E., 1948, Seismological Tables, British Association for the Advancement of Science, Gray Milne Trust.

Jordan, J.N., Black, R., and Bates, C.C., 1965A, "Patterns of Maximum Amplitudes of Pn and P Waves Over Regional and Continental Areas," B.S.S.A., Vol. 55, No. 4, pp. 693-720.

Jordan, J.N., Lander, J.F., and Black, R.A., 1965B, "Aftershocks of the 4 February 1965 Rat Island Earthquake," Science, Vol. 148, No. 3675, pp. 1323-1325.

Liebermann, R.C., King, Chi-Yu, Brune, J.N., and Pomeroy, P.W., 1966, "Excitation of Surface Waves by the Underground Nuclear Explosion LONGSHOT," J. Geophys. Res., Vol. 71, No. 18, pp. 4333-4339.

Murray, W.H., 1945, "Profiles of the Aleutian Trench," Geol. Soc. Amer. Bull., Vol. 56, pp. 757-782.

Oliver, J., Ewing, M., and Press, F., 1955, "Crustal Structure of the Arctic Regions from the Lg Phase," Geol. Soc. Amer. Bull., Vol. 66, pp. 1063-1074.

Oliver, J. and Isacks, B., 1967, "Deep Earthquake Zones, Anomalous Structures in the Upper Mantle, and Lithosphere," J. Geophys. Res., Vol. 72, No. 16, pp. 4259-4275.

Pakiser, L.C. and Zietz, I., 1965, "Transcontinental Crustal and Upper Mantle Structure," Review of Geophysics, Vol. 3, pp. 505-520.

Press, F. and Biehler, S., 1964, "Inferences on Crustal Velocities and Densities from P-wave Delays and Gravity Anomalies," J. Geophys. Res., Vol. 69, No. 14, pp. 2979-2995.

Romney, C., 1963, "An Investigation of the Relationship Between Magnitude Scales for Small Shocks," AFTAC Technical Report, VU-63-4, Project Vela Uniform.

Shor, G., 1964, "Structure of the Bering Sea and the Aleutian Ridge," Marine Geology, Vol. 1, pp. 213-219.

Sykes, L.R., 1966, "The Seismicity and Deep Structure of Island Arcs," J. Geophys. Res., Vol. 71, No. 12, pp. 2981-3006.

TABLE 1.--AMCHITKA Explosion, Arrival Times and Amplitudes of Principal Phases

Code	Station	Distance Km	Distance Degrees	Azimuth	Component	Phase	Observed Arrival Time 0200 Hrs. Min.	Observed Arrival Time 0200 Hrs. Sec.	Period T Sec.	Maximum Amplitude A/T (mu/sec)	Magnitude	J-B Residual	Remarks
ADK	Adak, Alaska	360.3	3.24	74.5	SPZ	ePn	08	02.5	0.6	166.6	5.0	-1.1	
					SPZ	e	08	03.9	---	---	---		Off scale
					SPZ	e	09	03.4	---	---	---		Off scale
SVW	Sparrevohn, Alaska	1943.8	17.48	45.1	SPZ	eP	11	18.5				+1.7	
KDC	Kodiak, Alaska	2012.7	18.10	57.2	SPZ	e(P)	11	22.7	0.4	60.0	4.7	-1.5	
					SPZ	ePP	11	33.1	0.9	65.2			
PMR	Palmer, Alaska	2289.6	20.59	46.9	SPZ	e(P)	11	51.1	0.7	13.4	4.2	-2.0	
					SPZ	e	11	53.4	0.7	24.6			
TNN	Tanana, Alaska	2316.3	20.83	35.9	SPZ	eP	11	55.7				+0.3	
SCM	Sheep Creek Mountain, Alaska	2389.7	21.49	46.9	SPZ	eP	12	00.4				-2.0	

TABLE 1.--(con.)

Code	Station	Distance Km	Distance Degrees	Azi-muth	Com-ponent	Phase	Observed Arrival Time 0200 Hrs. Min.	Observed Arrival Time 0200 Hrs. Sec.	Period T Sec.	Maximum Amplitude A/T (mu/sec)	Magni-tude	J-B Resid-ual	Remarks
COL	College, Alaska	2474.2	22.25	38.9	SPZ	eP	12	08.0	0.8	32.1	4.7	-1.6	
GIL	Gilmore Creek, Alaska	2490.9	22.40	38.8	SPZ	eP	12	08.7	0.8	12.5	4.3	-2.4	
PJD	Pedro Dome, Alaska	2492.0	22.41	38.6	SPZ	eP	12	10.2				-1.2	
BLR	Black Rapids, Alaska	2512.0	22.59	43.1	SPZ	eP	12	11.8				-1.4	
BH-	Burwash Landing Northwest Territories, Canada	2811.1	25.28	49.6	SPZ	eP	12	38.0	0.8	33.3	5.0	-1.2	

TABLE 1.--(con.)

Code	Station	Distance Km	Distance Degrees	Azi-muth	Com-ponent	Phase	Observed Arrival Time 0200 Hrs. Min.	Observed Arrival Time 0200 Hrs. Sec.	Period T Sec.	Maximum Amplitude A/T (mu/sec)	Magni-tude	J-B Resid-ual	Remarks
MBC	Mould Bay, Canada	3837.5	34.51	22.0	SPZ	eP	14	00.4				-0.7	
CMC	Coppermine, Canada	3954.3	35.56	36.8	SPZ	eP	14	09.0				-1.2	
YKC	Yellowknife, Canada	4086.6	36.75	45.7	SPZ	eP	14	18.5				-1.9	
PNT	Penticton, Canada	4301.2	38.68	67.6	SPZ	eP	14	35.2				-1.8	
LON	Longmire, Washington	4292.3	38.60	72.3	SPZ	e(P)	14	36.8				+0.4	
EDM	Edmonton, Canada	4501.4	40.48	59.4	SPZ	eP	14	49.8				-2.1	

TABLE 1.--(con.)

Code	Station	Distance Km	Distance Degrees	Azi-muth	Com-ponent	Phase	Observed Arrival Time 0200 Hrs. Min.	Sec.	Period T Sec.	Maximum Amplitude A/T (mu/sec)	Magni-tude	J-B Resid-ual	Remarks
NEW	Newport, Washington	4519.2	40.64	67.8	SPZ	eP	14	51.7	0.8	13.9	4.8	-1.6	
BMO	Blue Mountains Obs., Oregon	4701.5	42.28	72.4	SPZ	eP	15	05.9	0.7	9.7	4.5	-1.2	
					SPZ	ePcP	17	00.2	0.7	3.5			Poss. PP
MIN	Mineral, California	4688.2	42.16	80.6	SPZ	eP	15	06.2	(0.8)	13.8	4.6	0.0	
HHM	Hungry Horse, Montana	4713.8	42.39	66.2	SPZ	eP	15	06.4	0.6	3.2	4.0	-1.6	
ALE	Alert, Canada	4802.7	43.19	9.7	SPZ	eP	15	12.3				-0.9	
BLC	Baker Lake, Canada	4888.4	43.96	38.8	SPZ	eP	15	17.5				-2.3	

TABLE 1.--(con.)

Code	Station	Distance Km	Distance Degrees	Azi-muth	Com-ponent	Phase	Observed Arrival Time 0200 Hrs. Min.	Observed Arrival Time 0200 Hrs. Sec.	Period T Sec.	Maximum Amplitude A/T (mu/sec)	Magni-tude	J-B Resid-ual	Remarks
JAS	Jamestown, California	4928.4	44.32	82.6	SPZ SPZ	eP ePP	15 17	23.6 13.2	(0.8)	6.3	4.4	+0.1	 Poss. PcP
HL2	Hailey, Idaho	4972.9	44.72	72.3	SPZ	eP	15	27.0	0.8	22.5	5.0	0.0	
MN-	Mina, Nevada	5052.9	45.44	80.5	SPZ	eP	15	32.6	0.7	3.8	4.6	-0.3	
PRI	Priest, California	5036.2	45.29	84.7	SPZ	eP	15	33.2	(0.8)	5.0	4.4	+1.6	
EUR	Eureka, Nevada	5133.0	46.16	77.9	SPZ	eP	15	38.4	0.6	26.0	5.2	-0.5	
WDY	Woody, California	5194.2	46.71	83.9	SPZ	eP	15	42.0	0.6	1.6	4.1	-0.6	

TABLE 1.--(con.)

Code	Station	Distance Km	Distance Degrees	Azi-muth	Com-ponent	Phase	Observed Arrival Time 0200 Hrs. Min.	Observed Arrival Time 0200 Hrs. Sec.	Period T Sec.	Maximum Amplitude A/T (mu/sec)	Magni-tude	J-B Resid-ual	Remarks
LF4	Lasa-Sub-Array F4, Montana	5218.6	46.93	63.7	SPZ SPZ	iPc PcP	15 17	42.2 16.1	0.8	7.5	4.8	-1.9	
UBO	Uinta Basin, Utah	5510.0	49.55	72.9	SPZ	eP	16	04.1	0.9	5.5	4.5	-0.8	
KN-	Kanab, Utah	5517.7	49.62	78.4	SPZ	eP	16	05.3	0.6	4.0	4.3	-0.2	
GLA	Glamis, California	5666.8	50.96	83.7	SPZ	eP	16	14.9				-0.6	
RK-	Red Lake, Canada	5791.3	52.08	53.4	SPZ	eP	16	20.7	0.8	9.7	4.7	-2.8	
GOL	Golden, Colorado	5832.4	52.45	71.0	SPZ	eP	16	25.0	0.7	4.1	4.3	-2.0	

TABLE 1.--(con.)

Code	Station	Distance Km	Distance Degrees	Azi-muth	Com-ponent	Phase	Observed Arrival Time 0200 Time Min.	Observed Arrival Time 0200 Time Sec.	Period T Sec.	Maximum Amplitude A/T (mu/sec)	Magni-tude	J-B Resid-ual	Remarks
TFO	Tonto Forest Obs., Arizona	5823.5	52.37	80.0	SPZ	eP	16	25.5	0.7	2.0	4.0	-0.9	
TUC	Tucson, Arizona	6002.6	53.98	81.5	SPZ	eP	16	36.7	0.9	4.4	4.4	-1.6	
ALQ	Albuquerque, New Mexico	6103.8	54.89	76.1	SPZ	eP	16	43.4	0.9	4.3	4.4	-1.6	
GWC	Great Whale River, Canada	6295.0	56.61	41.7	SPZ	eP	16	53.6				-2.9	
LC-	Las Cruces, New Mexico	6283.9	56.51	78.5	SPZ	eP	16	57.7	0.7	7.3	4.7	+1.0	

TABLE 1.--(con.)

Code	Station	Distance Km	Distance Degrees	Azi-muth	Com-ponent	Phase	Observed Arrival Time 0200 Hrs. Min.	Observed Arrival Time 0200 Hrs. Sec.	Period T Sec.	Maximum Amplitude A/T (mu/sec)	Magni-tude	J-B Resid-ual	Remarks
WMO	Wichita Mountain Obs., Oklahoma	6649.8	59.80	71.1	SPZ	eP	17	18.0	0.6	7.0	4.6	-1.5	
					SPZ	e	17	30.8	0.5	3.8			
					SPZ	e	17	36.0	0.5	4.3			
					SPZ	ePcP	18	06.2	0.6	5.0			
SV3	Schefferville, Canada	6819.9	61.33	36.8	SPZ	eP	17	26.4	0.7	21.5	5.1	-3.0	
CPO	Cumberland Plateau, Tennessee	7415.9	66.69	61.9	SPZ	eP	18	04.5	0.6	11.7	5.1	-0.5	
HN-	Houlton, Maine	7507.1	67.51	43.6	SPZ	eP	18	07.2	0.8	8.3	4.9	-2.6	
SHL	Shillong, India	7606.1	68.40	284.2	SPZ	ePc	18	14.3	0.7	12.4	5.1	-1.7	

TABLE 1.--(con.)

Code	Station	Distance Km	Distance Degrees	Azi-muth	Com-ponent	Phase	Observed Arrival Time 0200 Hrs. Min.	Observed Arrival Time 0200 Hrs. Sec.	Period T Sec.	Maximum Amplitude A/T (mu/sec)	Magni-tude	J-B Resid-ual	Remarks
WES	Weston, Mass.	7666.1	68.94	48.1	SPZ	eP	18	16.8	0.8	9.0	5.0	-1.9	
KBL	Kabul, Afghanistan	8292.2	74.57	306.1	SPZ	eP	18	51.4	0.8	12.9	4.9	-1.5	
CTA	Charter Towers, Australia	8485.7	76.31	210.9	SPZ	eP	19	02.8				+0.3	
WRA	Warramunga, Australia	8964.9	80.62	221.5	SPZ	eP	19	25.4				-0.8	
PRE	Pretoria, South Africa	15229.6	145.95	306.8	SPZ SPZ	ePKP ePcPP'	26 38	53.2 26.4	0.7 1.0	16.4 27.0		+0.4	

TABLE 1.--(con.)

Code	Station	Distance Km	Distance Degrees	Azi-muth	Com-ponent	Phase	Observed Arrival Time 0200 Hrs. Min.	Observed Arrival Time 0200 Hrs. Sec.	Period T Sec.	Maximum Amplitude A/T (mu/sec)	Magni-tude	J-B Resid-ual	Remarks
WIN	Windhoek, South Africa	16456.5	147.99	325.9	SPZ	ePKP	26	59.2	0.6	5.4		+3.0	
					SPZ	e(PcsP')	38	44.7	1.1	0.2			

WORLD-WIDE STANDARD SEISMOGRAPH STATIONS UNDERLINED.
FOR STATION COORDINATES SEE C&GS "SEISMOGRAPH STATION ABBREVIATIONS" BOOK.
e=EMERGENT; i=IMPULSIVE; c=COMPRESSION; ( )=DOUBTFUL VALUES OR PHASES;
- DENOTES LRSM STATIONS

TABLE 2.--Travel-Time Residuals Related to Tectonic Provinces

Sta	Western Orogenic Belt LONGSHOT/AMCHITKA		Sta	Canadian Shield and Central Stable Interior LONGSHOT/AMCHITKA		Sta	Appalachian Belt LONGSHOT/AMCHITKA	
BH-	-3.5	-1.2	MBC	-3.4	-0.7	HN-	-5.7	-2.6
PNT	-3.9	-1.8	CMC	-3.4	-1.2	WES	-5.2	-1.9
LON	-3.0	-0.4	YKC	-4.2	-1.9	CPO	-5.3	-0.5
BMO	-3.4	-1.2	EDM	-4.4	-2.1		-5.40*	-1.67*
HHM	-3.0	-1.6	ALE	-3.5	-0.9			
JAS	-1.8	+0.1	BLC	-4.4	-2.3			
HL2	-3.1	0.0	LASA	-4.8	-1.9			
MN-	-2.1	-0.3	RK-	-5.6	-2.8			
EUR	-2.3	-0.5	SV3	-1.0	-3.0			
WDY	-2.8	-0.6	WMO	-4.3	-1.5			
KN-	-2.1	-0.2		-3.90*	-1.83*			
TFO	-2.8	-0.9						
TUC	-3.3	-1.6						
ALQ	-3.8	-1.6						
LC-	-3.4	+1.0						
UBO	-3.2	-0.8						
GOL	-3.7	-2.0						
	-3.01*	-0.80*						

*Similar station average mean residual

TABLE 3.--Magnitude Residuals at Stations Which Recorded AMCHITKA and LONGSHOT

Sta	Western Orogenic Belt LONGSHOT/AMCHITKA		Sta	Canadian Shield and Central Stable Interior LONGSHOT/AMCHITKA		Sta	Appalachian Belt LONGSHOT/AMCHITKA	
BH-	-0.3	+0.4	SV3	+0.3	+0.5	CPO	+0.2	+0.5
BMO	-0.4	-0.1	WMO	-0.2	0.0	HN-	+0.5	+0.3
HHM	-0.6	-0.6	RK-	+0.2	+0.1		+0.35*	+0.40*
JAS	-0.3	-0.2	LASA	+0.3	+0.2			
MN-	-0.4	0.0		+0.15*	+0.20*			
HL2	0.0	+0.4						
EUR	+0.5	+0.6						
KN-	-0.2	-0.3						
TUC	0.0	-0.2						
ALQ	+0.1	-0.2						
LC-	-0.3	+0.1						
GOL	-0.2	-0.3						
UBO	+0.6	-0.1						
	-0.12*	-0.04*						

*Mean magnitude residual of group

TABLE 4.--Hypocentral Solutions - AMCHITKA Explosion

Solution No.	Station No.	Depth km.	Origin Time	Coordinates Lat.°	Long.°	Shift (km) From Actual Location Lat.	Long.	Shift Directions
1#	51	*0	*02 07 10.40	*51.125N	*178.367E	---	---	--
2#	49	37	02 07 15.12	51.298N	178.354E	19.24	0.91	NW
3#	48	*0	02 07 09.51	51.288N	178.285E	18.13	5.76	NW
4##	48	*0	02 07 12.09	51.259N	178.287E	14.91	5.62	NW
5**	38	33	02 07 18.4	51.202N	178.506E	8.56	9.76	NE
6**	38	*0	02 07 13.1	51.168N	178.432E	4.78	4.56	NE

#Jeffreys-Bullen curve used in computation.

##Herrin curve used in computations.

*Data input--parameters restrained.

**Arrival times adjusted with the use of LONGSHOT residuals (Jeffreys-Bullen curve).

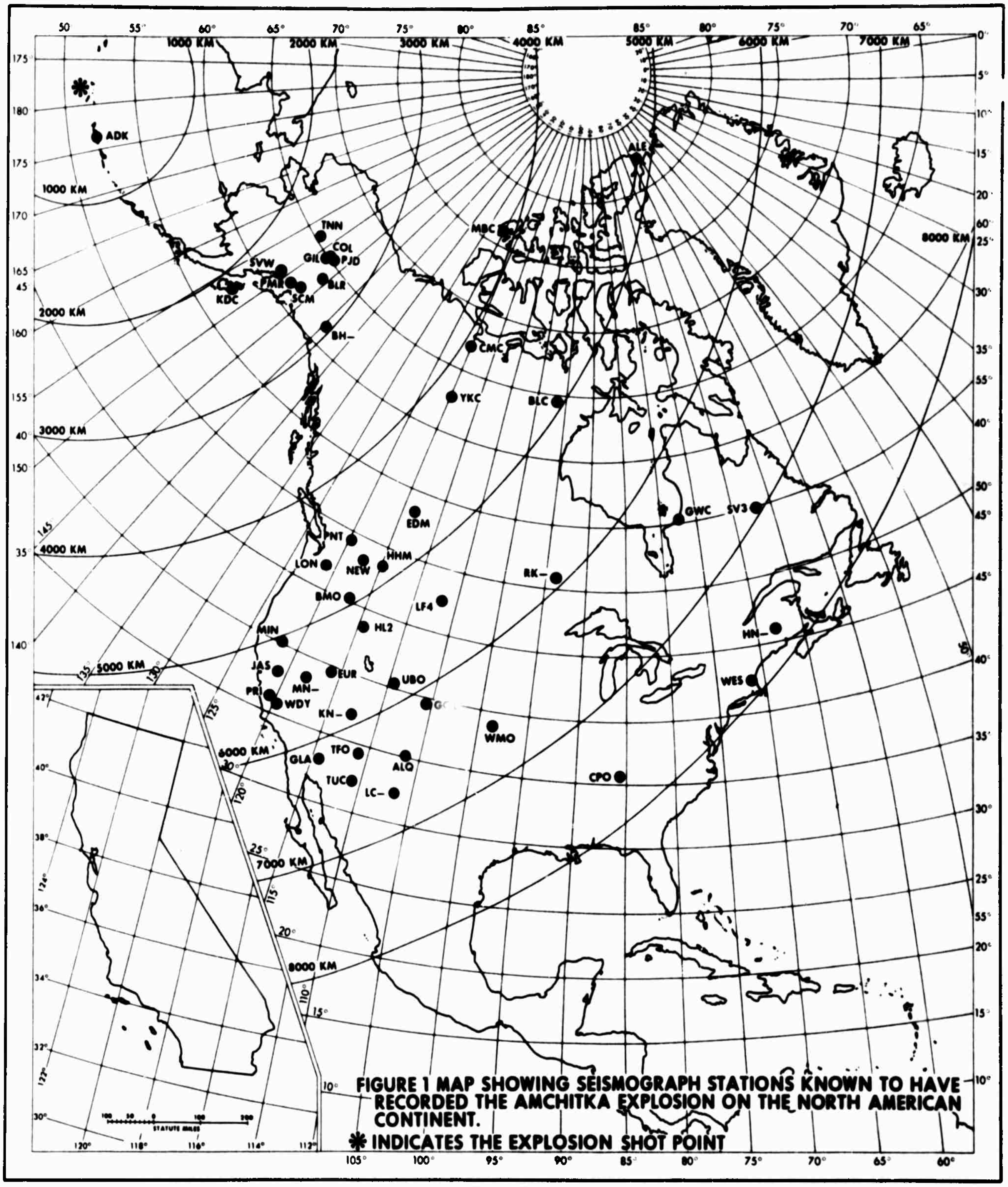

FIGURE 1 MAP SHOWING SEISMOGRAPH STATIONS KNOWN TO HAVE RECORDED THE AMCHITKA EXPLOSION ON THE NORTH AMERICAN CONTINENT.

✱ INDICATES THE EXPLOSION SHOT POINT

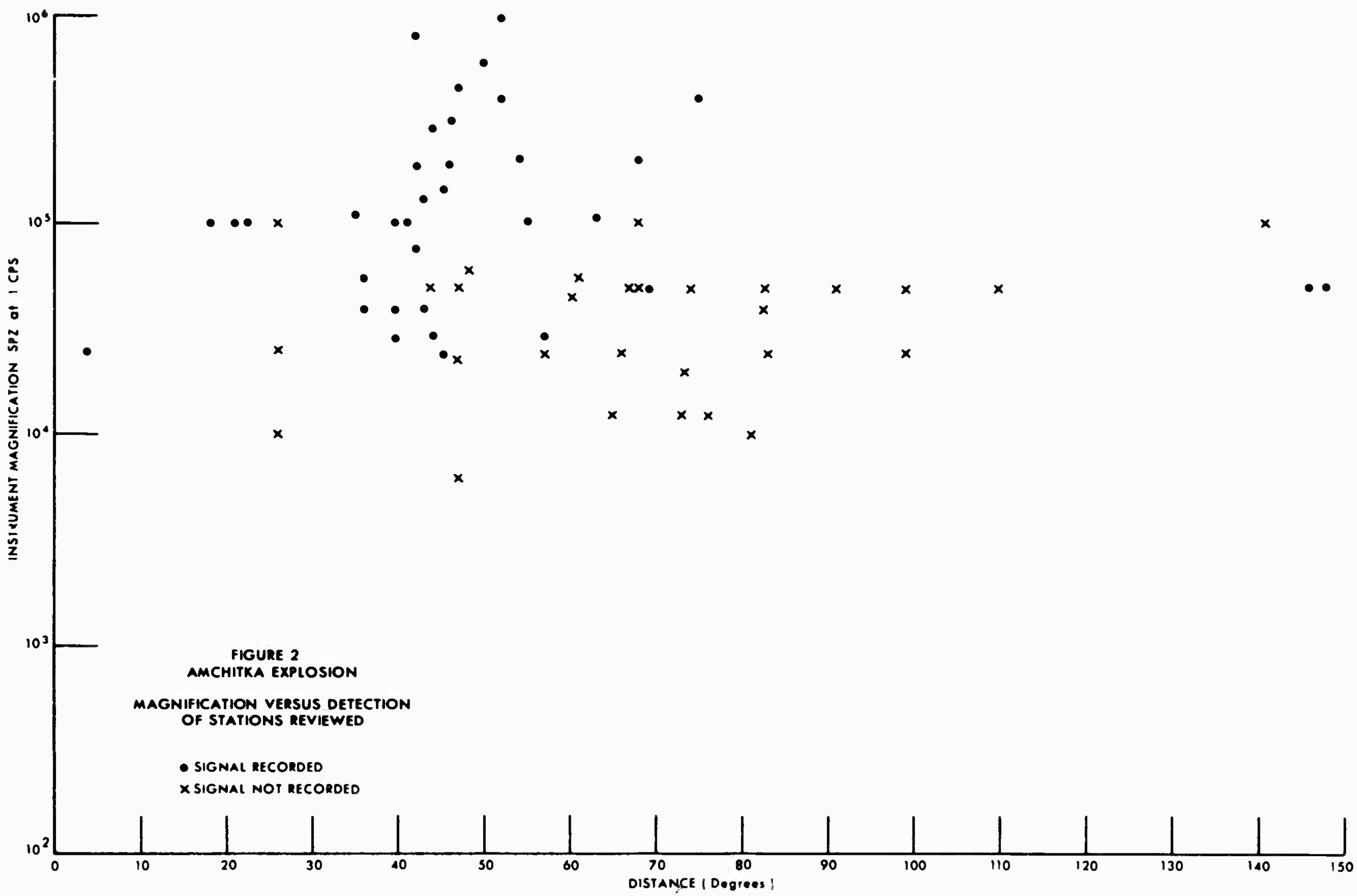

FIGURE 2
AMCHITKA EXPLOSION

MAGNIFICATION VERSUS DETECTION
OF STATIONS REVIEWED

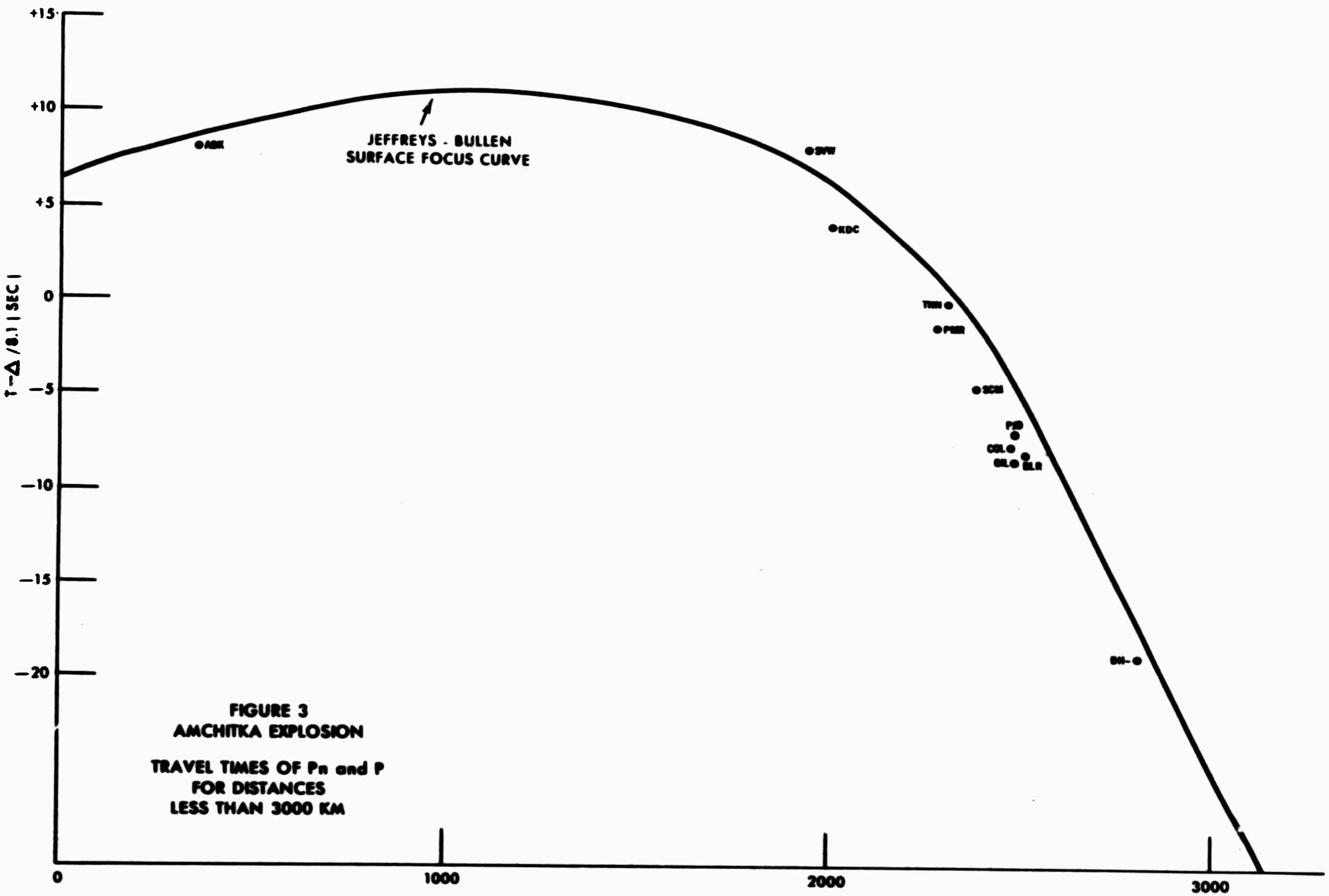

FIGURE 3
AMCHITKA EXPLOSION

TRAVEL TIMES OF Pn and P
FOR DISTANCES
LESS THAN 3000 KM

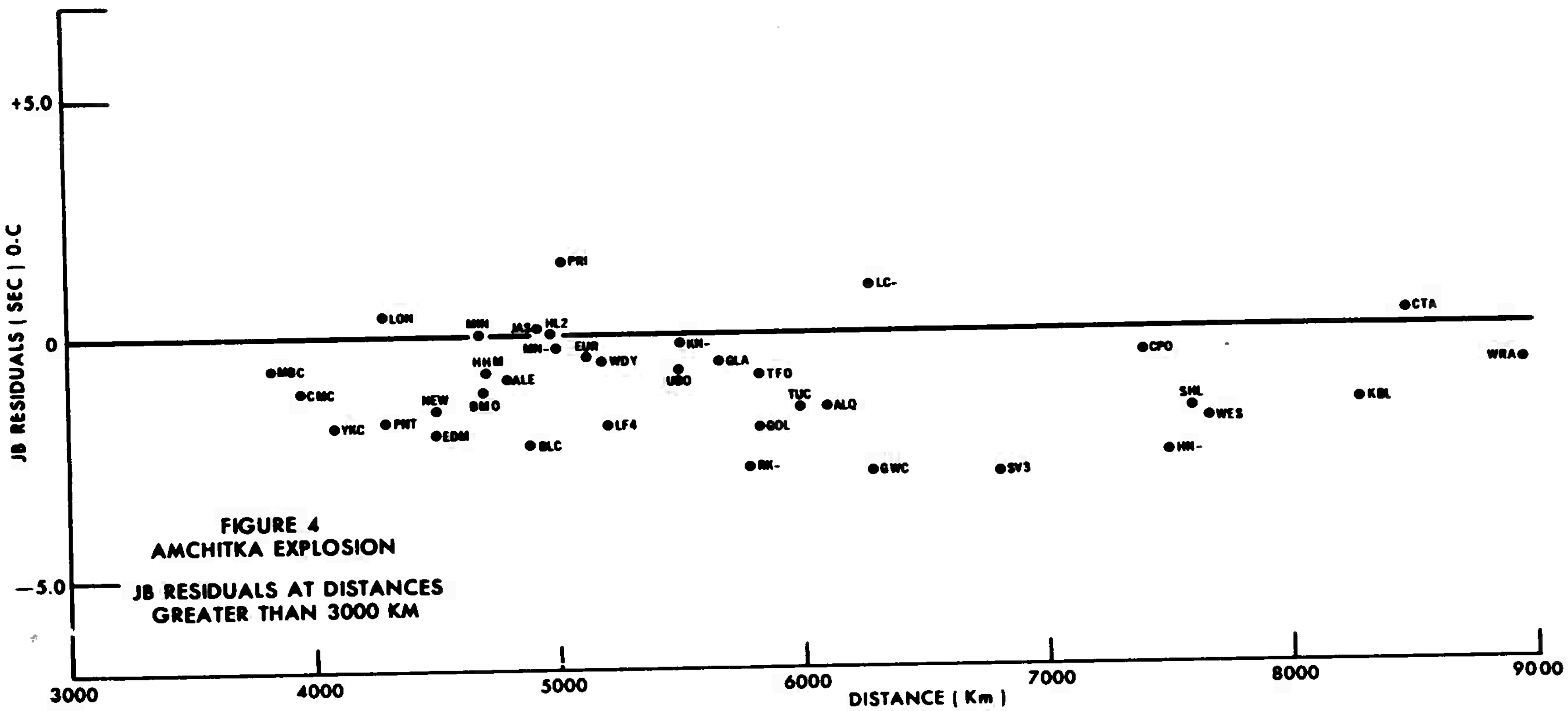

FIGURE 4
AMCHITKA EXPLOSION
JB RESIDUALS AT DISTANCES
GREATER THAN 3000 KM

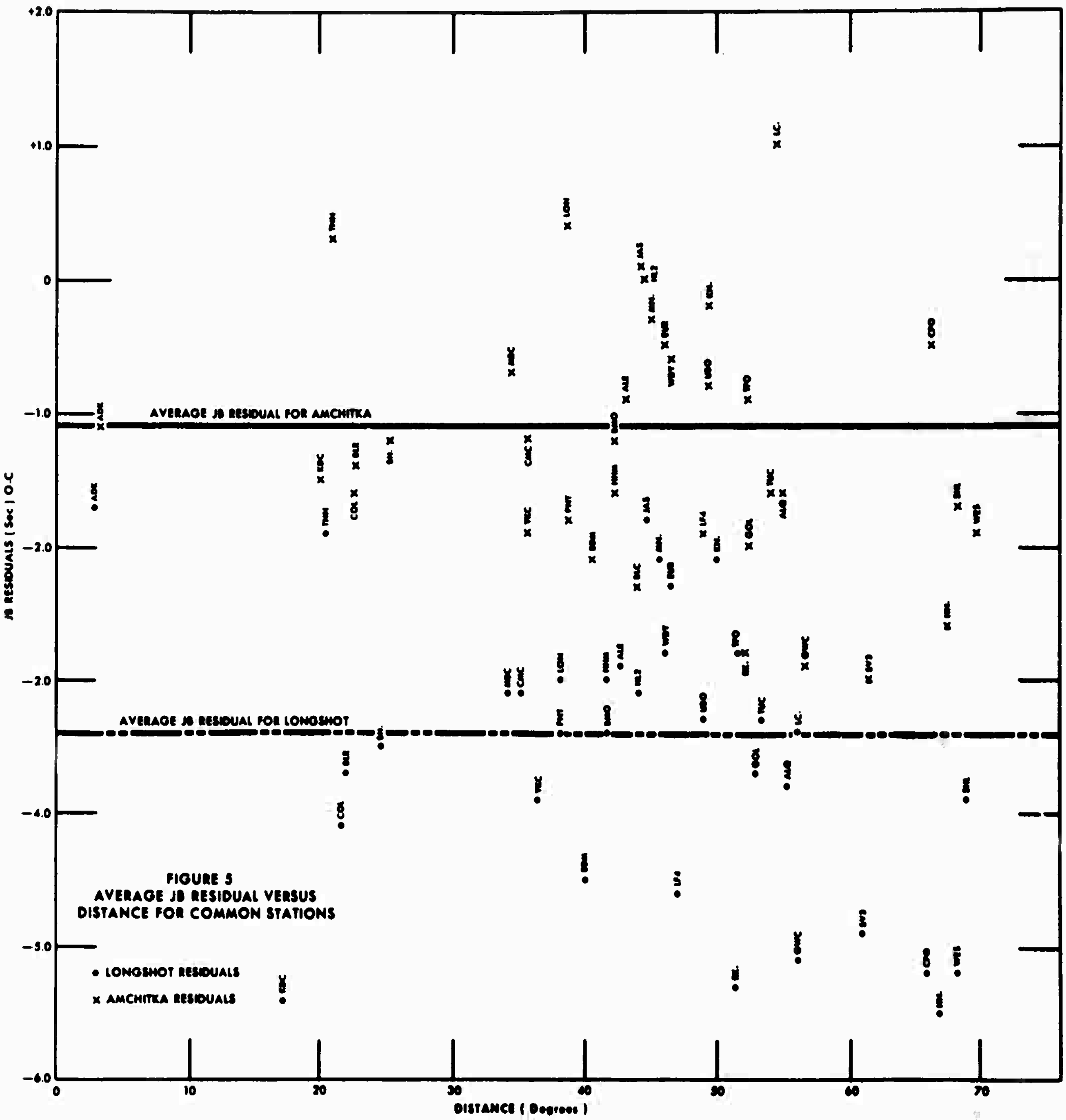

FIGURE 5
AVERAGE JB RESIDUAL VERSUS
DISTANCE FOR COMMON STATIONS

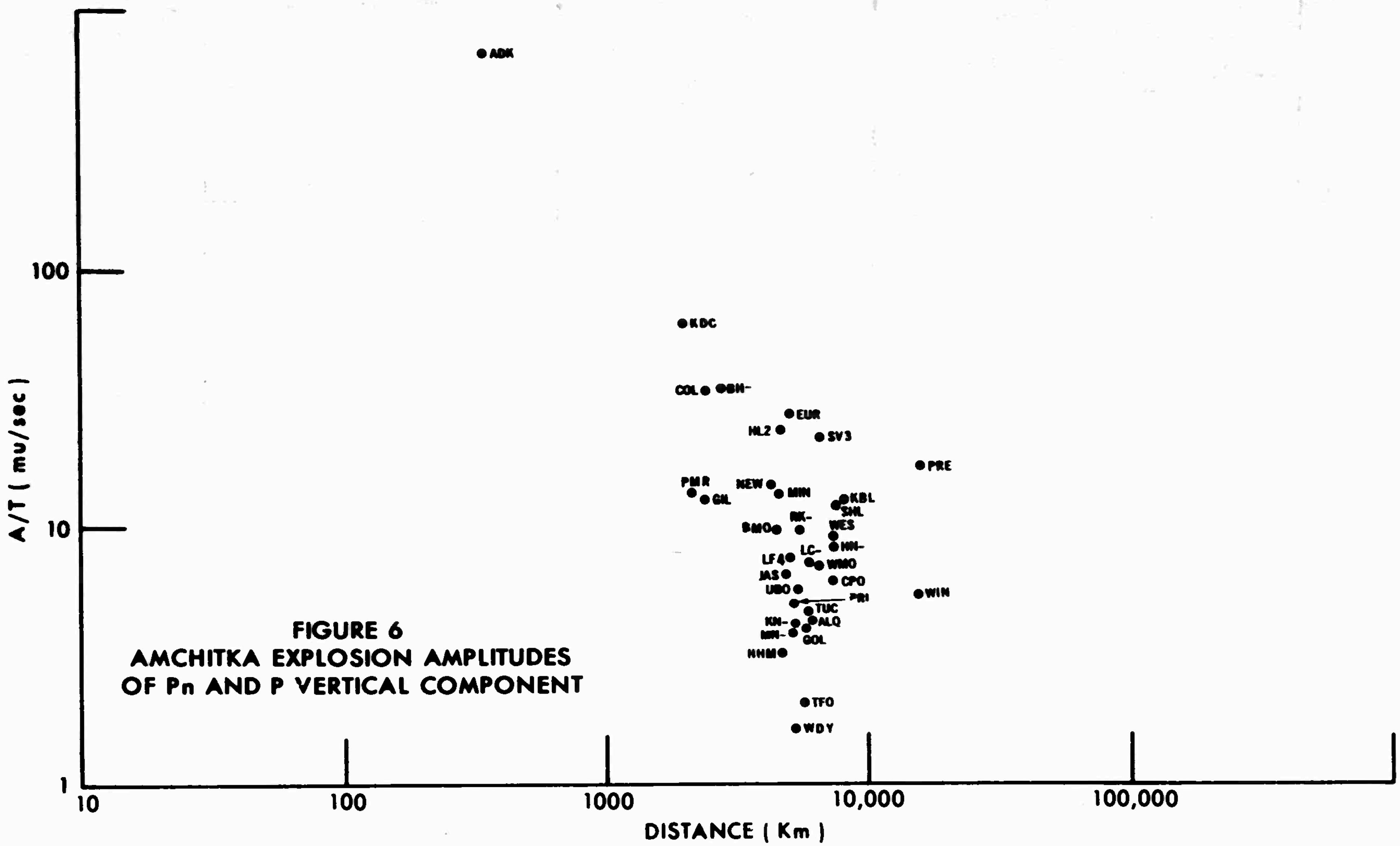

FIGURE 6
AMCHITKA EXPLOSION AMPLITUDES
OF Pn AND P VERTICAL COMPONENT

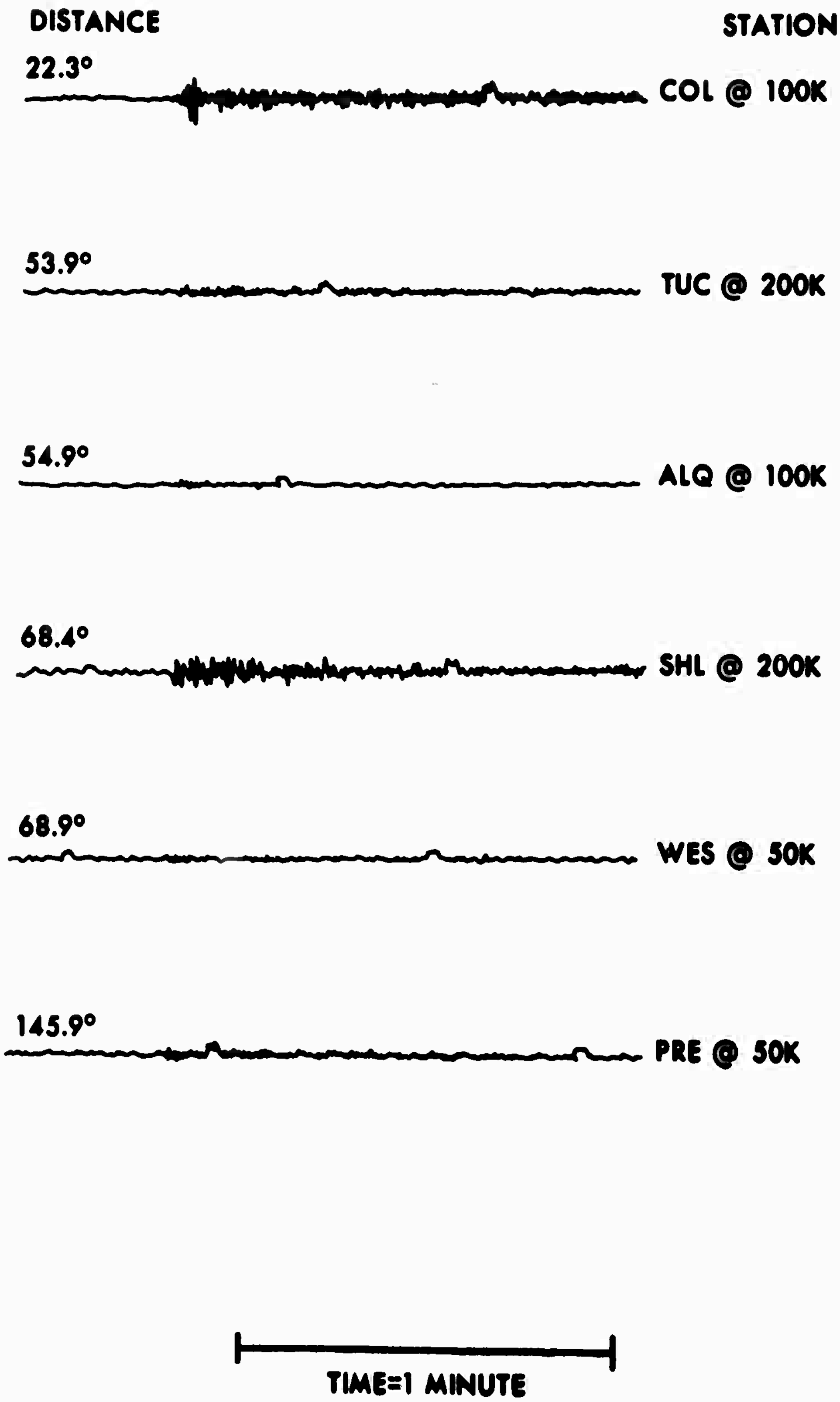

FIGURE 7 REPRESENTATIVE SIGNALS RECORDED FROM THE AMCHITKA EXPLOSION

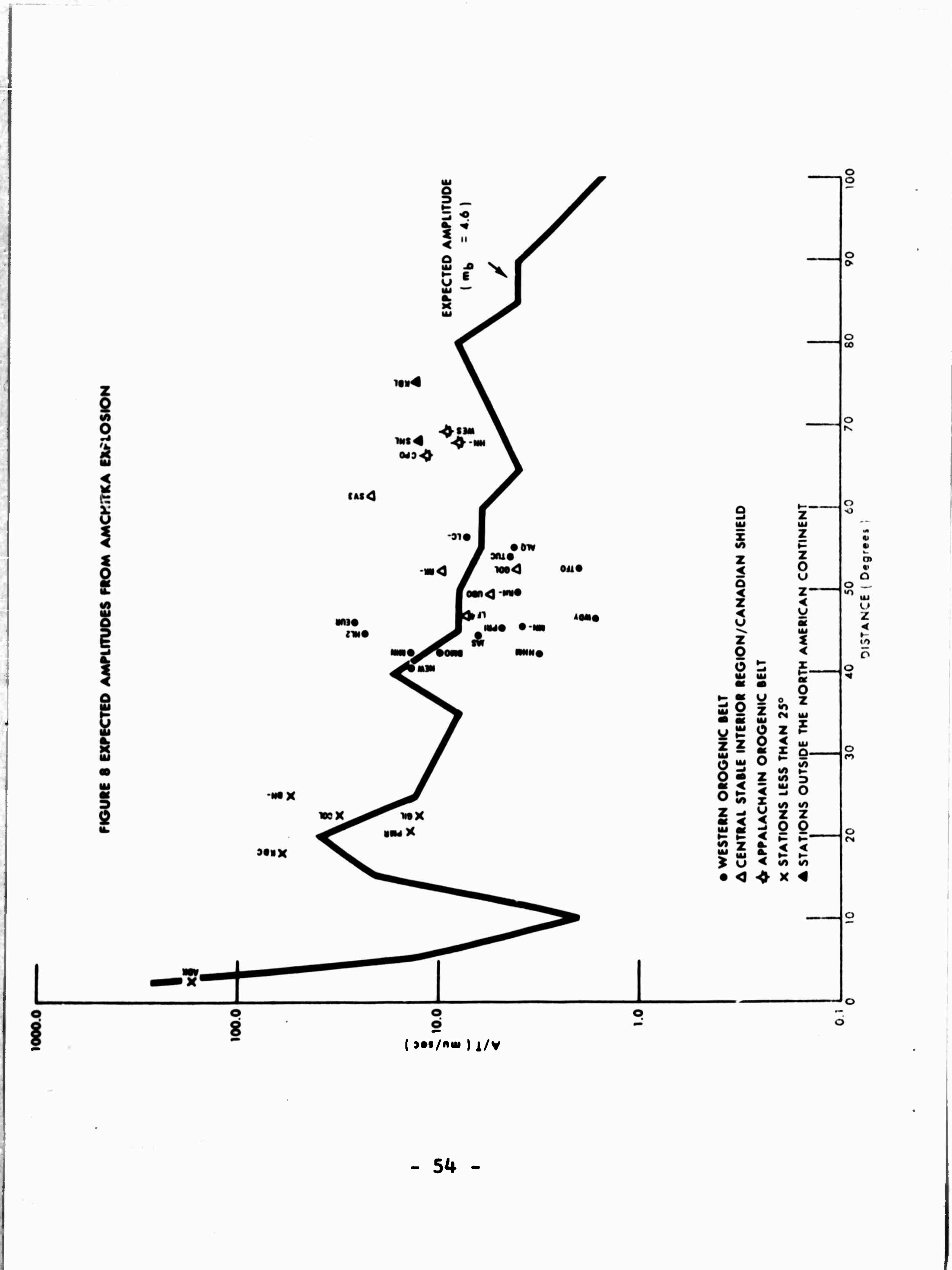

FIGURE 8 EXPECTED AMPLITUDES FROM AMCHITKA EXPLOSION

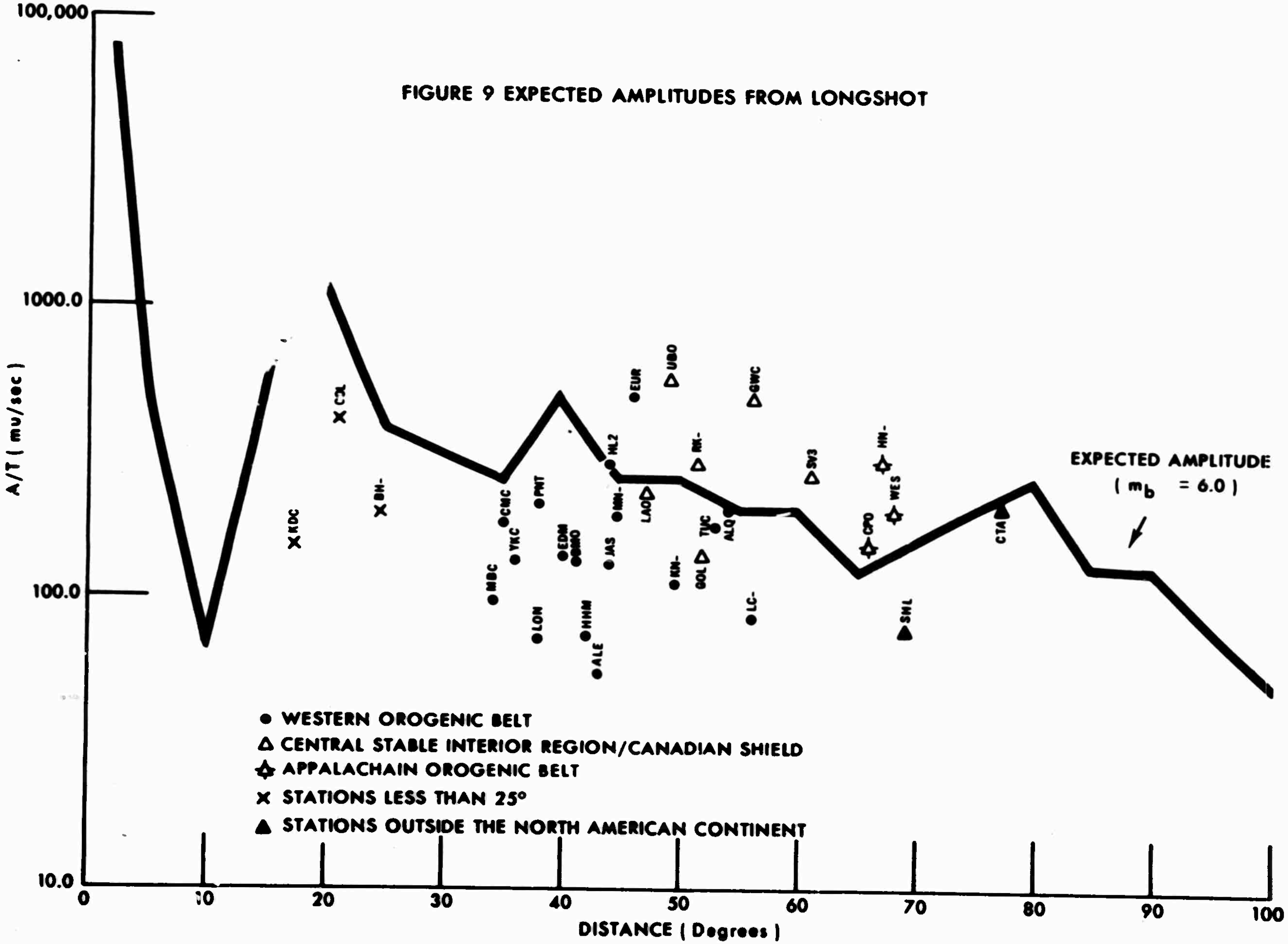

FIGURE 9 EXPECTED AMPLITUDES FROM LONGSHOT

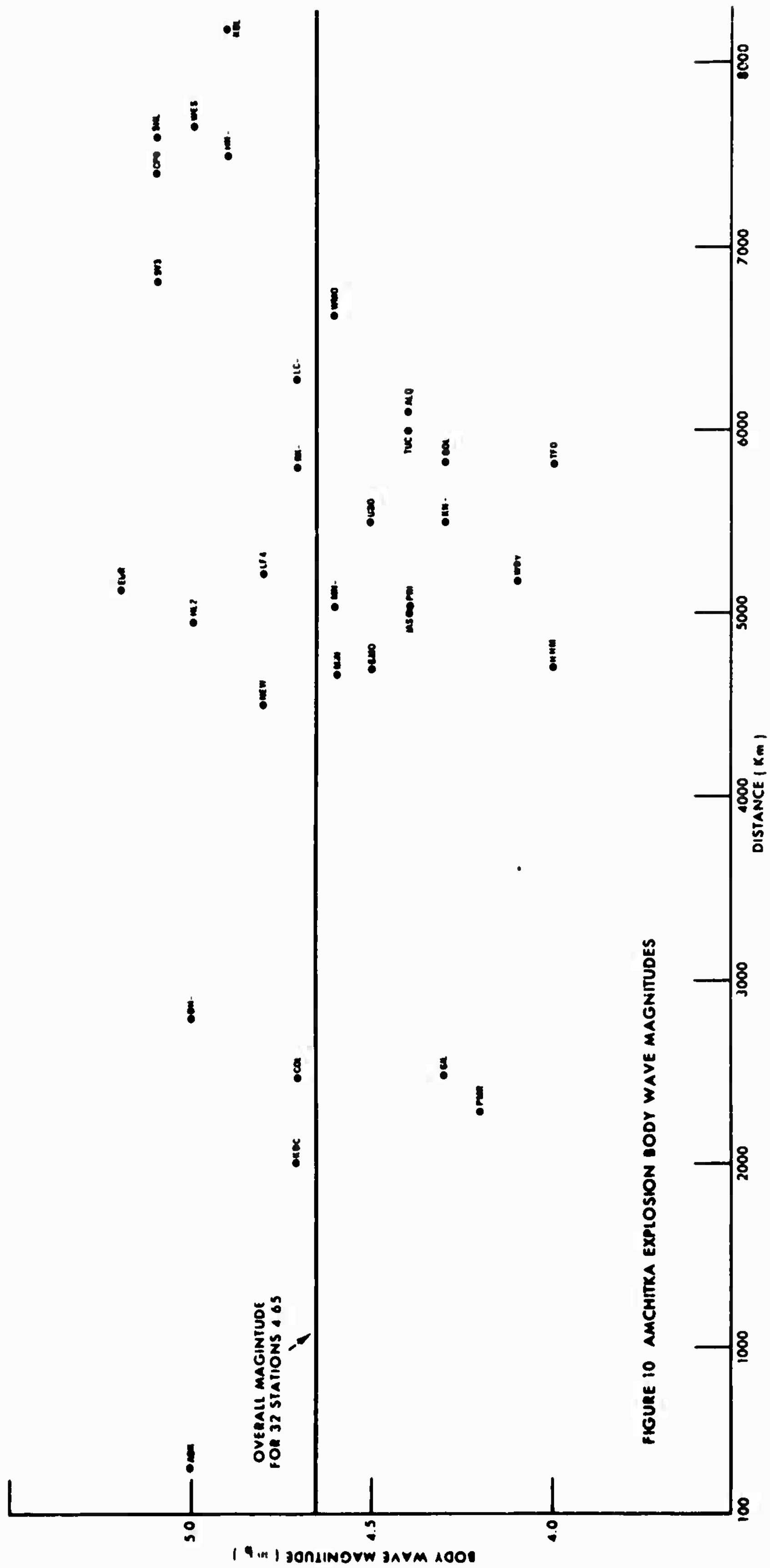

FIGURE 10 AMCHITKA EXPLOSION BODY WAVE MAGNITUDES

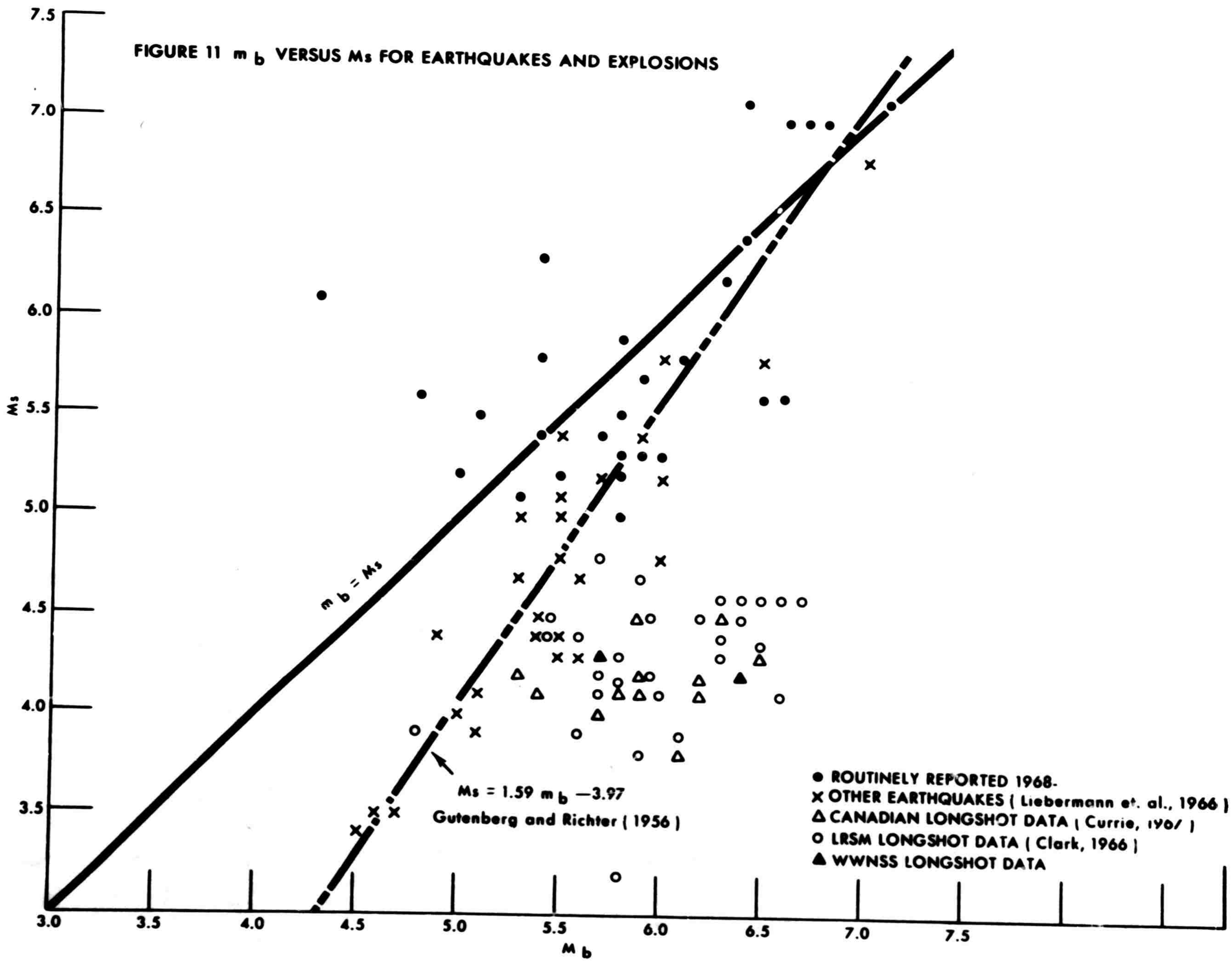

FIGURE 11 m_b VERSUS M_s FOR EARTHQUAKES AND EXPLOSIONS

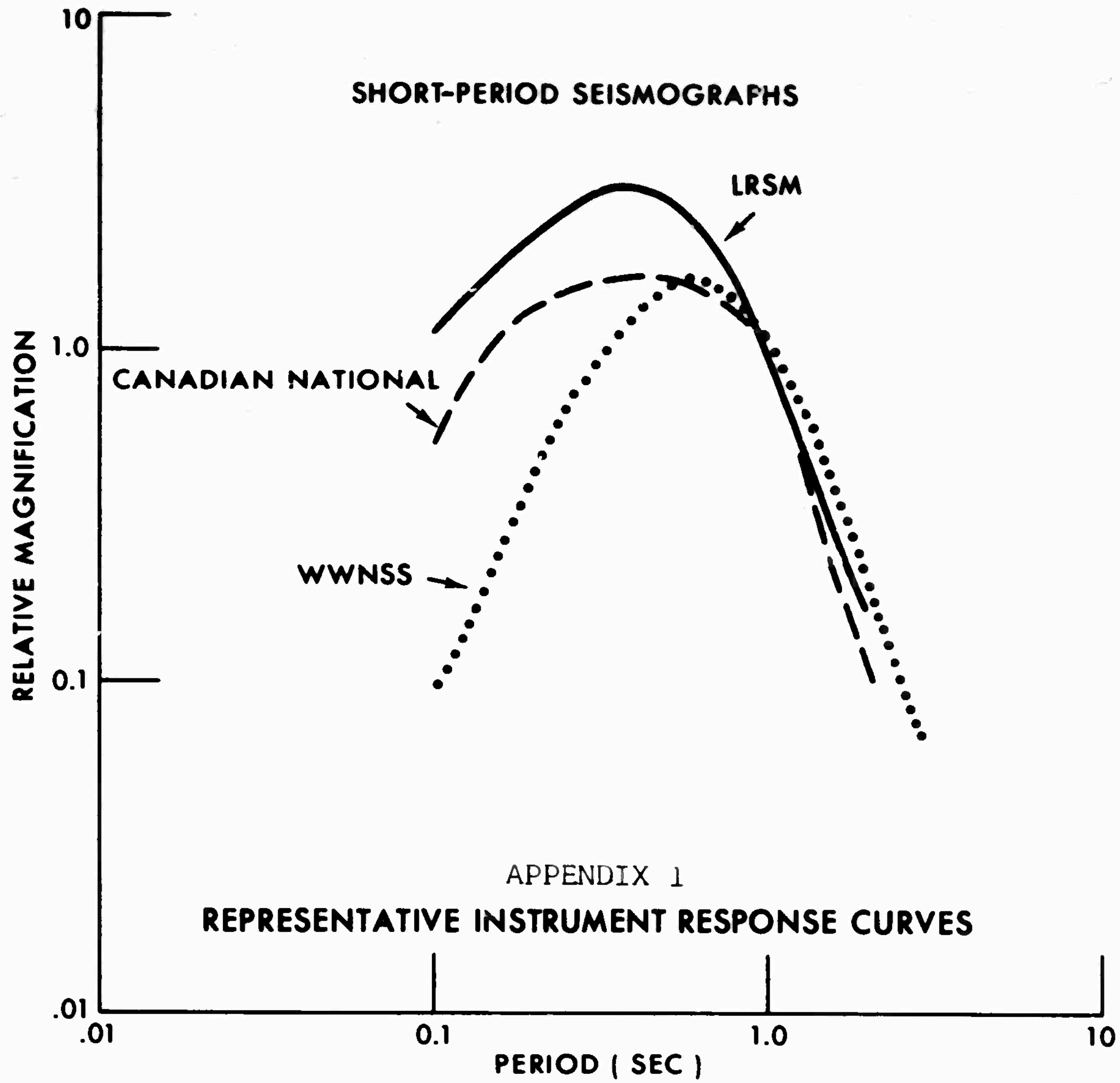

APPENDIX 1

REPRESENTATIVE INSTRUMENT RESPONSE CURVES

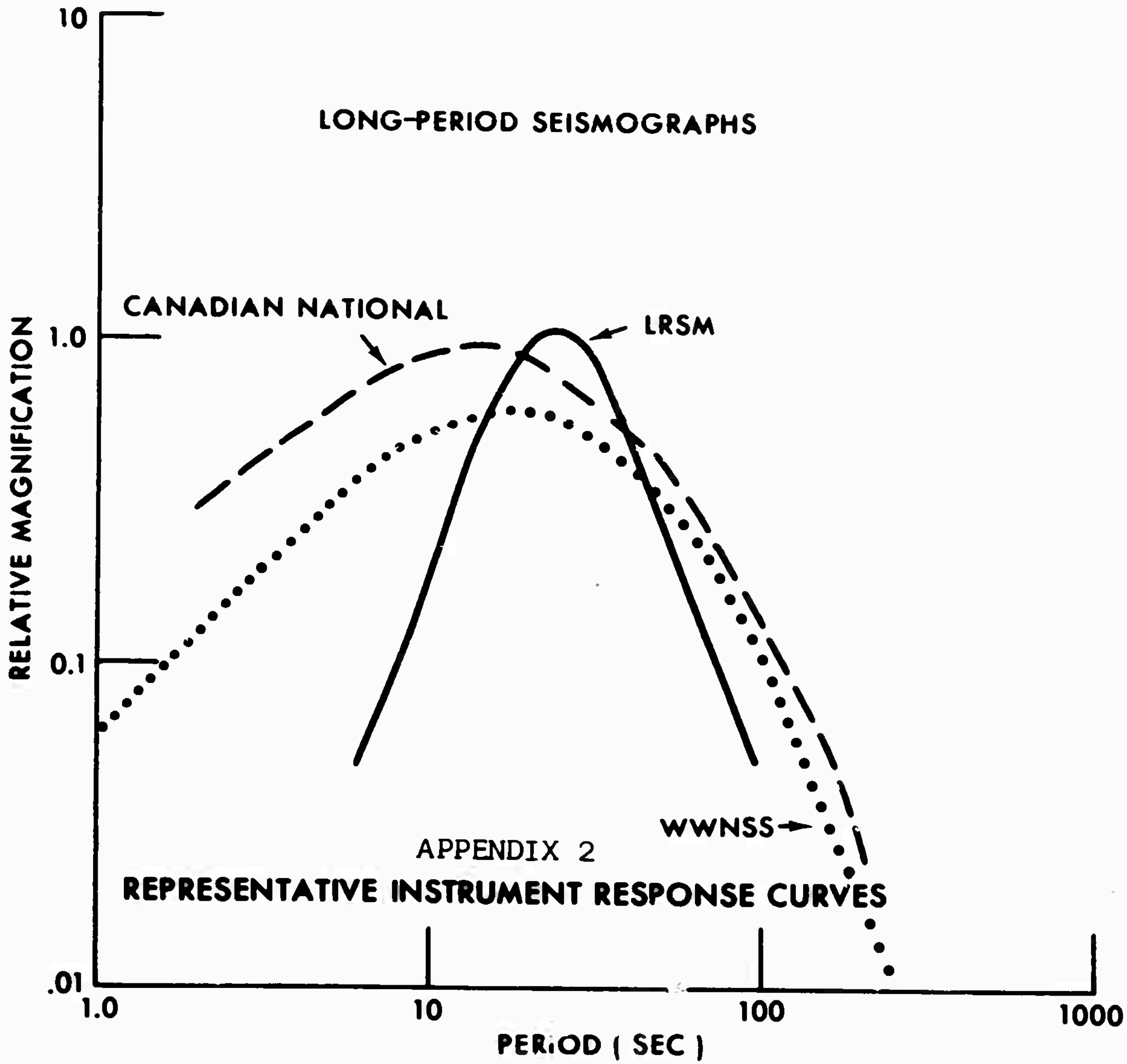

APPENDIX 2

REPRESENTATIVE INSTRUMENT RESPONSE CURVES